Multitarget Tracking with the von Mises-Fisher Filter and Probabilistic Data Association

IVAN MARKOVIĆ
MARIO BUKAL
JOSIP ĆESIĆ
IVAN PETROVIĆ

Directional data emerge in many scientific disciplines due to the nature of the observed phenomena or the working principles of a sensor. The problem of tracking with direction-only sensors is challenging since the motion of the target typically resides either in 3D or 2D Euclidean space, while the corresponding measurements reside either on the unit sphere or the unit circle, respectively. Furthermore, in multitarget tracking there is the need to deal with the problem of pairing sensors measurements with targets in the presence of clutter (the data association problem). In this paper we propose to approach multitarget tracking in clutter with direction-only data by setting it on the unit hypersphere, thus tracking the objects with a Bayesian estimator based on the von Mises-Fisher distribution and probabilistic data association. To achieve this goal we derive the probabilistic data association (PDA) filter and the joint probabilistic data association (JPDA) filter for the Bayesian von Mises-Fisher estimation on the unit hypersphere. The final PDA and JPDA filter equations are derived with respect to the Kullback-Leibler divergence by preserving the first moment of the hyperspherical distribution. Although the fundamental equations are given for the hyperspherical case, we focus on the filters on the unit 1-sphere (circle in $\mathbb{R}^2$) and the unit 2-sphere (surface of the unit ball in $\mathbb{R}^3$). The proposed approach is validated through synthetic data experiments on 100 Monte Carlo runs simulating multitarget tracking with noisy directional measurements and clutter.

Manuscript received February 2, 2016; released for publication March 10, 2016.

Refereeing of this contribution was handled by Igor Gilitschenski.

Authors' address: I. Marković, J. Ćesić, I. Petrović, Department of Computer and Control Engineering, University of Zagreb, Faculty of Electrical Engineering and Computing, Zagreb, Croatia. (E-mail: {ivan.markovic, josip.cesic, ivan.petrovic}@fer.hr). M. Bukal, Department of Applied Mathematics, University of Zagreb, Faculty of Electrical Engineering and Computing, Zagreb, Croatia. (E-mail: mario.bukal@fer.hr).

This is an extended version of the paper *Direction-only tracking of moving objects on the unit sphere via probabilistic data association* published at the *17th International Conference on Information Fusion (FUSION2014).*

This work has been supported by the European Regional Development Fund under the project *Advanced Technologies in Power Plants and Rail Vehicles.*

I. INTRODUCTION

Directional data emerge in many scientific disciplines. Since the surface of the earth is approximately a sphere, such data arise readily in earth sciences, e.g. the location of the earthquake's epicenter, the paleomagnetic directions of the earth's magnetic pole etc. Furthermore, many astronomical observations are points on the celestial sphere and as such yield directional data. In multitarget tracking (MTT), it is not uncommon to work with sensors that can provide only directions to the objects in question. The measurement and estimation state space have a specific geometry of their own, which is different from the true trajectory space geometry.

The problem is challenging, because, although the motion of the target resides either in 3D or 2D Euclidean space, corresponding measurements reside either on the sphere or the circle, respectively. For example, if we are measuring and estimating only the direction to the target in 2D, i.e. the azimuth, the state and measurements will bear the non-Euclidean properties of angles. Applying standard filtering techniques employing the Gaussian distribution on $\mathbb{R}^d$ would ignore the underlying geometry. In robotics, measurements from various sensors, due to their nature of operation, yield direction-only information of the objects of interest, e.g. microphone arrays measure the direction of the sound source, perspective and omnidirectional cameras measure directions of various features of interest in space.

Considering MTT, the goal of such a system is to estimate the multiple trajectories in scenarios with noisy measurements, clutter or false alarms (measurements that falsely appear to originate from moving objects). The duties of such a system are truly numerous, and in the past several seminal methods have been developed in order to tackle this problem wherein data association plays one of the crucial roles. To solve this problem the methods that can be used are the global nearest neighbor (GNN) which attempts to find the single most likely data association hypothesis at each scan [1], the probabilistic data association (PDA) filter for single target tracking and joint probabilistic data association (JPDA) filter for MTT where multiple hypotheses are formed after each scan and then these hypotheses are combined before proceeding further with the next scan [2], and the multiple hypothesis filter (MHT) [3] where multiple data association hypotheses are formed and propagated from scan to scan [1]. Furthermore, a group of methods based on random finite sets was developed with MTT in mind. An example is the probability hypothesis density (PHD) filter [4] which estimates the number of objects in the scene but does not solve the data association problem by itself, however, a solution has been presented in [5] for the Gaussian mixture PHD filter [6]. Further solutions within this framework were developed, such as the cardinalized PHD (CPHD) [7], [8], and multi-Bernoulli filters [9]–[12].

Estimation methods using the von Mises (vM) and the wrapped Gaussian distributions were recently discussed in [13]–[22]. Furthermore, inference on quaternions, namely the Bingham distribution (which actually models variables with 180° symmetry), was used in [23]–[25] and in [26] where, furthermore, a second-order filter was derived which included also the rotational velocity. These approaches, advocating the unit hypersphere as the appropriate filtering space, showed better performance of the Bingham filter compared to the extended Kalman filter. This approach was further extended to unscented orientation estimation based on the Bingham distribution and showed better performance than the unscented Kalman filter and better to equal performance than the particle filter (depending on the number of particles) [27]. However, the normalization constant of the Bingham distribution, hence its partial derivative, cannot be computed in closed form, but this can be surmounted by caching techniques and its relationship with the vM distribution [25]. On the contrary, the von Mises-Fisher (vMF) distribution does not require such techniques since the normalization constant and its partial derivative can be calculated in closed form, which will be of practical interest in the ensuing JPDA equations. Indeed, there are many choices for directional distributions, but for inferential purposes the vMF distribution is most widely used because of its exponential family structure [28].

Considering target tracking on the unit sphere (as in surface of the unit ball in $\mathbb{R}^3$), it was proposed in [29] to utilize the vMF distribution to model the system state and the sensors measurements after which a Bayesian estimator was developed for single object tracking. This method was used in our previous work [30] in order to track a single target detected by an omnidirectional camera on a mobile robot, thus not offering a consistent method for dealing with multiple moving objects nor false alarms/clutter. A global nearest neighbor (GNN), which in contrast to JPDA solves the data association by hard assignment, was applied in tracking multiple targets on the sphere in [31] and the Rényi α-divergence was used as a distance measure. In [32] we developed the vM mixture PHD filter and compared it to the Gaussian mixture PHD filter for MTT on the unit circle. The vM mixture PHD filter showed better performance since it was able to capture the circle geometry intrinsically, which proved important for the mixture PHD filter having components spread throughout the entire state space. In [33] the vMF filter was used to track multiple speakers. The authors also addressed modeling the object velocity with a Gaussian distribution by assuming that the posterior state distribution can factor to the product of the vMF and the Gaussian distribution. The authors compared the performance of the vMF filter to the constant velocity Kalman filter and a particle filter based on the vMF sampling. The vMF filter showed better performance than the Kalman filter, while the performance with respect to the vMF particle filter depended on the number of particles (at the cost of increase in computational complexity). Multitarget tracking was solved by averaging observations prior to the update step, where the weights were computed based on the normalized vMF innovation term (also taking into account a uniform distribution to handle outliers). The authors conclude that the vMF filter strikes a good compromise between the efficiency of the Kalman filter and the statistical grounding of the vMF particle filter.

In [34] we proposed a probabilistic data association solution to the problem of tracking single and multiple targets in clutter with direction-only sensors. This papers serves as a foundation for the present paper and we are extending it in several ways. Instead of focusing on the unit sphere, in the present work the Bayesian filter is presented on the unit hypersphere, i.e. the $(d-1)$-dimensional unit sphere, and it is shown how vM and vMF filters arise as special cases. We also provide in depth mathematical proofs of the moment-matching techniques used in the paper. Furthermore, validation gating is discussed in detail and experiments are extended through more thorough validation via MC runs of the vM and vMF PDA and JPDA filters.

Specifically, we pose the problem on the unit hypersphere and utilize a Bayesian tracking algorithm that is based on the vMF distribution on the $(d-1)$-dimensional unit sphere. To solve the data association problem we derive the PDA and JPDA filter equations for the aforementioned Bayesian filter. This constituted (i) deriving the a posteriori probabilities of association events on the unit hypersphere which essentially weigh each hypothetical estimation and form a mixture of von Mises-Fisher densities, (ii) determining the final (single) component density as the result of the update in the PDA and JPDA filter by preserving the first moment of the hyperspherical distribution (which is optimal in the Kullback-Leibler sense), and (iii) modeling the false alarms as Poisson processes. The proposed algorithms were tested on 100 Monte Carlo runs of a synthetic data set comprising of single and multiple-object scenarios where direction-only measurements were corrupted with noise and clutter.

The paper is organized as follows. Section II presents the general mathematical background and formulae for tracking on the hypersphere with the von Mises-Fisher distribution. Section III describes the proposed PDA and JPDA filtering approaches based on the von Mises-Fisher distribution. Section IV presents the results and discussion of the synthetic data experiments, while Section V concludes the paper.

II. GENERAL BACKGROUND

When considering directions in d dimensions, i.e. unit vectors in d-dimensional Euclidean space $\mathbb{R}^d$, one can represent them as points on the $(d-1)$-dimensional sphere $\mathbb{S}^{d-1}$ of unit radius. Thus, in our notation, 1-sphere is the unit circle in $\mathbb{R}^2$ and the 2-sphere is

the surface of the unit ball in $\mathbb{R}^3$. In the sequel we introduce all the necessary constituents and discuss the basic paradigm of a tracking system on the unit $(d-1)$-sphere using von the Mises-Fisher distributions.

A. von Mises-Fisher distribution

Parametric probability distribution defined on the unit $(d-1)$-dimensional sphere $\mathbb{S}^{d-1}$, whose probability density function (pdf) is given by

$$f(\mathbf{x};\boldsymbol{\mu},\kappa) = C_d(\kappa)\exp(\kappa\boldsymbol{\mu}\cdot\mathbf{x}), \quad \mathbf{x}\in\mathbb{S}^{d-1}, \tag{1}$$

is called *von Mises-Fisher distribution* with parameters $\kappa \geq 0$ and $\boldsymbol{\mu}\in\mathbb{S}^{d-1}$ denoting the concentration and the mean direction, respectively. Expression

$$C_d(\kappa) = \frac{\kappa^{d/2-1}}{(2\pi)^{d/2} I_{d/2-1}(\kappa)} \tag{2}$$

is the normalization constant with respect to the standard surface measure, while I_p denotes the modified Bessel function of the first kind and order p [35]. To enlighten many of its properties, it is worth of considering the vMF distributions as an exponential family. Recall, a parametric set of probability distributions parametrized by the natural parameter $\boldsymbol{\theta}\in\boldsymbol{\Theta}\subseteq\mathbb{R}^d$ is called an *exponential family* if their probability densities admit the following canonical representation [36]

$$p(\mathbf{x};\boldsymbol{\theta}) = \exp(T(\mathbf{x})\cdot\boldsymbol{\theta} - F(\boldsymbol{\theta}) + C(\mathbf{x})), \tag{3}$$

where $T(\mathbf{x})$ is called sufficient statistics, $F(\boldsymbol{\theta})$ is the log-normalizing function and $C(\mathbf{x})$ denotes the carrier measure. Many familiar parametric distributions, like the Gaussian, Poisson, Gamma, Dirichlet etc., are exponential families [37].

One easily deduces from (1) that the vMF distribution constitutes an exponential family parametrized by the natural parameter $\boldsymbol{\theta} = \kappa\boldsymbol{\mu}\in\mathbb{R}^d$, the log-normalizing function given by

$$F_d(\boldsymbol{\theta}) = -\log C_d(\|\boldsymbol{\theta}\|), \tag{4}$$

and the trivial carrier measure. The minimal sufficient statistics is the identity map on $\mathbb{S}^{d-1}$, $T(\mathbf{x}) = \mathbf{x}$, hence, the vMF distribution is completely determined by the *directional (angular) mean*[1]

$$\mathbb{E}[\mathbf{x}] = \int_{\mathbb{S}^{d-1}} \mathbf{x} f(\mathbf{x};\boldsymbol{\mu},\kappa) d\mathbf{x} = \nabla F_d(\boldsymbol{\theta}) = A_d(\kappa)\boldsymbol{\mu}, \tag{5}$$

where $A_d(\kappa)$ is the ratio of the following Bessel functions

$$A_d(\kappa) = \frac{I_{d/2}(\kappa)}{I_{d/2-1}(\kappa)}. \tag{6}$$

Please see Proposition A.1 in Appendix A for the proof. Let us mention two more distinctive properties of the vMF distribution: (i) density (1) is rotationally invariant around the mean direction and, (ii) analogously to the multivariate Gaussian distribution, it is characterized by the *maximum entropy principle* in the following sense. Given any pdf on $\mathbb{S}^{d-1}$ of prescribed directional mean $\boldsymbol{\eta}$, it is then the vMF distribution with the natural parameter $\boldsymbol{\theta} = (\nabla F)^{-1}(\boldsymbol{\eta})$, which maximizes the Boltzmann-Shannon entropy $-\int_{\mathbb{S}^{d-1}} p(\mathbf{x})\log p(\mathbf{x}) d\mathbf{x}$ [29, Proposition 2.2].

In the present paper we present the vMF filter on $\mathbb{S}^{d-1}$, but due to the aimed application of MTT, we particularly show explicit relation in cases when $d = 2$ and $d = 3$, i.e. the vMF distributions on the unit 1-sphere (called the von Mises distribution) and the unit 2-sphere (also called the Fisher or Langevin distribution). For the former the above expressions amount to [35]

$$C_2(\kappa) = \frac{1}{2\pi I_0(\kappa)} \quad \text{and} \quad A_2(\kappa) = \frac{I_1(\kappa)}{I_0(\kappa)}, \tag{7}$$

while for the latter they simplify to

$$C_3(\kappa) = \frac{\kappa}{4\pi\sinh\kappa} \quad \text{and} \quad A_3(\kappa) = \frac{1}{\tanh\kappa} - \frac{1}{\kappa}. \tag{8}$$

An example of von Mises-Fisher distributions on the unit 1-sphere and the unit 2-sphere with different mean directions and concentration parameters are depicted in Fig. 1 and Fig. 2, respectively. Even though the application examples are shown for cases when $d = 2$ and $d = 3$, with the presented general approach the higher dimensional von Mises-Fisher filter could be applied in novel applications beyond MTT. For example, a higher dimensional von Mises-Fisher distribution was used in [38] to address large scale data mining applications, such as text categorization and gene expression analysis, which involve high-dimensional data that is also inherently directional in nature.

Please note that we will denote the 1-sphere Bayes filter as the von Mises filter, while with the practical slight abuse of terminology the 2-sphere Bayes filter will be denoted as the von Mises-Fisher filter and where necessary the general Bayes filter on the $(d-1)$-sphere will be called the hyperspherical von Mises-Fisher filter. Furthermore, all the explicit formulae for the vM distribution will be presented in angular variables with the following relation $\boldsymbol{\mu} = (\cos\alpha, \sin\alpha)$.

B. Motion model

In our model we assume that moving objects are relatively slow with respect to the sampling rate, i.e. changes in the objects's position between two consequent observations are relatively small. Mathematically, motion of such objects is then described by a wide-sense stationary stochastic processes, among which, the Wiener process (Brownian motion) is the standard choice [39]. These time-continuous processes are typically further approximated by a random walk of a fixed time step.

The Brownian motion distribution on $\mathbb{S}^{d-1}$ with parameters $\boldsymbol{\mu}$ and κ is the distribution at time κ^{-1} of a random point which starts at $\boldsymbol{\mu}$ and moves on $\mathbb{S}^{d-1}$ under

[1] Note that the *directional mean* is defined by the integral (5), while the *mean direction* $\boldsymbol{\mu}$ is the parameter of the von Mises-Fisher distribution.

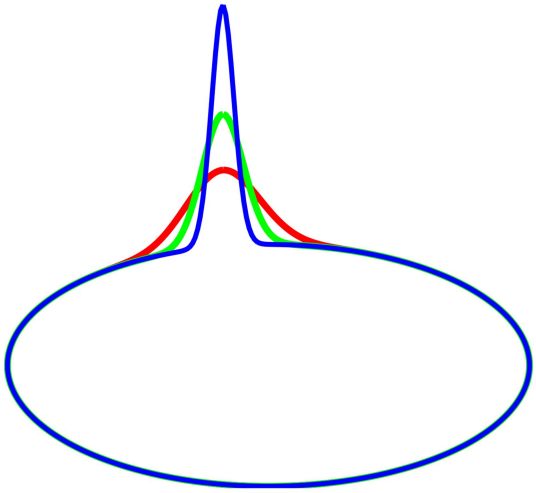

Fig. 1. Examples of the von Mises-Fisher distribution on the unit 1-sphere, i.e. the von Mises distribution, with equal mean directions and concentration parameters of 50 (red), 150 (green), and 500 (blue), which correspond approximately to standard deviations of 8.1°, 4.7° and 2.6°, respectively.

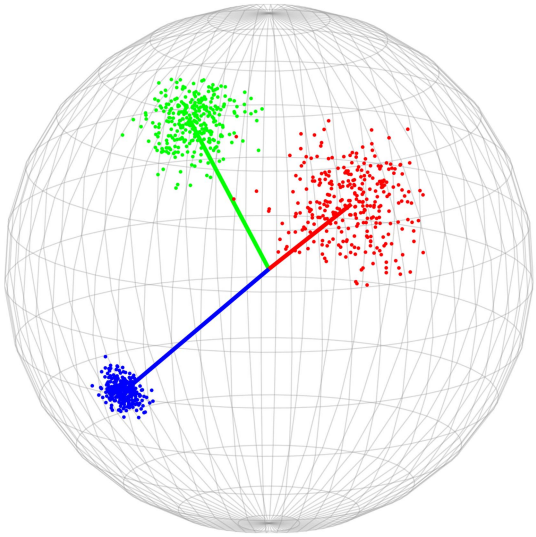

Fig. 2. Samples on the unit 2-sphere of the von Mises-Fisher distribution with different mean directions and concentration parameters of 50 (red), 150 (green), and 500 (blue), which correspond approximately to standard deviations of 10°, 5.7° and 3.1°, respectively.

an isotropic diffusion with infinitesimal variance $\mathbf{I}_{d-1}$ (the identity matrix on the tangent space of $\mathbb{S}^{d-1}$) [28]. When $d = 2$ the Brownian motion distribution is the wrapped Normal distribution, which in turn is very close to and can be well approximated by the von Mises distribution with corresponding parameter transformations [16], [28]. This closeness of the densities also extends to the distributions on $\mathbb{S}^{d-1}$, i.e. to the Brownian motion distribution and the von Mises-Fisher distribution on $\mathbb{S}^{d-1}$, as we shall detail out in the sequel for $d = 3$. In practice, this means that in the prediction stage we can approximate Brownian motion well with the corresponding vMF distribution.

When $d = 3$, there are at least two viewpoints which motivate the vMF as a motion model. First, consider an isotropic Wiener process (Brownian motion) on $\mathbb{S}^2$, which is defined as a temporally and spatially homogeneous Markov process [40]. It has been shown that such process exists and is unique. Moreover, the pdf of the distribution of a random point starting at $\hat{\mathbf{x}}^{k-1} \in \mathbb{S}^2$ and moving to $\hat{\mathbf{x}}^k$ at time $\tau > 0$ is given by

$$p(\hat{\mathbf{x}}^k \mid \hat{\mathbf{x}}^{k-1}) = \frac{1}{4\pi} \sum_{l=0}^{\infty} (2l+1) e^{-\tau l(l+1)/4} L_l(\hat{\mathbf{x}}^{k-1} \cdot \hat{\mathbf{x}}^k), \quad (9)$$

where L_l are Legendre polynomials of degree l. This formula is also obtained as the limit of the vanishing step size of a random walk on the sphere with all directions of movement being equally probable [41]. Furthermore, in the same paper the authors discuss the approximation of (9), which is the true $\mathbb{S}^2$-analogue of the planar symmetric Gaussian distribution, by a von Mises-Fisher distribution, which unlike (9) features certain analyticity properties. They show that for small variance $\tau > 0$, one can approximate the Brownian motion on $\mathbb{S}^2$ by the von Mises-Fisher diffusion with large concentration parameter $\kappa_\tau = 2/\tau$, i.e.

$$p(\hat{\mathbf{x}}^k \mid \hat{\mathbf{x}}^{k-1}) \approx f(\hat{\mathbf{x}}^k; \hat{\mathbf{x}}^{k-1}, \kappa_\tau).$$

The second approach is from the applicational viewpoint probably even more relevant. Consider the isotropic Wiener process in $\mathbb{R}^3$ and corresponding time-discretization (random walk) of fixed time step $\tau > 0$. The transition probability density function of the process is given by the Gaussian density

$$p(\mathbf{x}^k \mid \mathbf{x}^{k-1}) = \frac{1}{(2\pi\sigma_\tau^2)^{3/2}} \exp(-\|\mathbf{x}^k - \mathbf{x}^{k-1}\|^2 / 2\sigma_\tau^2), \quad (10)$$

where $\sigma_\tau^2 := \sigma^2 \tau$ and $\sigma > 0$ denotes the process strength. If we are confined to a measurement device which only measures direction $\hat{\mathbf{x}}^k \in \mathbb{S}^2$ of position vectors $\mathbf{x}^k$, then marginalizing (10) over the range, one obtains statistical model being the *angular Gaussian* density [42]

$$p(\hat{\mathbf{x}}^k \mid \mathbf{x}^{k-1}) = \frac{1}{C} \int_0^\infty s^2 \exp(-s^2/2\kappa_\tau + s\hat{\mathbf{x}}^{k-1} \cdot \hat{\mathbf{x}}^k) ds \quad (11)$$

with parameters $\hat{\mathbf{x}}^{k-1} = \mathbf{x}^{k-1}/\|\mathbf{x}^{k-1}\|$, $\kappa_\tau = \|\mathbf{x}^{k-1}\|^2/\sigma_\tau^2$, and normalization constant C. Following [29], for moderate or large values of κ_τ (practically most relevant cases), (11) can be well approximated by the vMF density $f(\hat{\mathbf{x}}^k; \hat{\mathbf{x}}^{k-1}, \kappa_\tau)$.

Usage of physically more realistic motion models like Ornstein-Uhlenbeck or Langevin processes [43], in place of simple Wiener process, requires more complex state representation manifolds and solving the Fokker-Planck equation to obtain the corresponding state transition densities. The latter typically needs to be further approximated by an appropriate parametric density which

will keep the model computationally tractable and statistically consistent with the remaining ingredients of the filtering algorithm: state distribution and measurement model.

C. Observation model

As already announced above, we assume that observation process consists of measuring a direction, where measurement disturbances are interpreted as random rotations, i.e. observed direction $\mathbf{z}$ is a random rotation of the true direction $\mathbf{x}$. It is reasonable to statistically describe such model by a unimodal distribution which is rotationally invariant around the true direction $\mathbf{x}$.

Since our goal is to derive a Bayesian filter on $\mathbb{S}^{d-1}$, our choice for the measurement model will be the von Mises-Fisher distribution defined on the $(d-1)$-sphere, represented by its density

$$p(\mathbf{z} \mid \mathbf{x}) = C_d(\kappa_o)\exp(\kappa_o \mathbf{x}\cdot\mathbf{z}), \quad \mathbf{z},\mathbf{x}\in\mathbb{S}^{d-1}, \tag{12}$$

where the concentration parameter κ_o describes the measurement uncertainty. In the present paper specific examples will be given when $d = 2$ and $d = 3$, serving as a model for representing measurements of directions, i.e. angle-only measurements, in 2D and 3D Euclidean spaces.

D. Bayesian filter equations

With a Bayes filter we are striving to estimate the density $p(\mathbf{x}^k \mid \mathbf{z}^{1:k})$, i.e. the pdf of the sate $\mathbf{x}^k$ at time instant k given the history of all the measurements $\mathbf{z}^{1:k}$. This process can be decomposed in two steps—namely the prediction and the correction step. Let us assume that at time instant $k-1$ we have estimated the pdf of the targeted state, i.e. we have the available the posterior $p(\mathbf{x}^{k-1} \mid \mathbf{z}^{1:k-1})$. For the case at hand, filtering on $\mathbb{S}^{d-1}$, the prediction step amounts to solving the following integral

$$p(\mathbf{x}^k \mid \mathbf{z}^{1:k-1}) = \int_{\mathbb{S}^{d-1}} p(\mathbf{x}^k \mid \mathbf{x}^{k-1})p(\mathbf{x}^{k-1} \mid \mathbf{z}^{1:k-1})d\mathbf{x}^{k-1}, \tag{13}$$

where $p(\mathbf{x}^k \mid \mathbf{x}^{k-1})$ is the transition density or motion model of the tracked object. Then, after receiving the measurement at time instant k the correction step amounts to evaluating the Bayes rule

$$p(\mathbf{x}^k \mid \mathbf{z}^{1:k}) = \frac{p(\mathbf{z}^k \mid \mathbf{x}^k)p(\mathbf{x}^k \mid \mathbf{z}^{1:k-1})}{p(\mathbf{z}^k \mid \mathbf{z}^{1:k-1})}, \tag{14}$$

where $p(\mathbf{z}^k \mid \mathbf{x}^k)$ is the sensor model and the normalizer $p(\mathbf{z}^k \mid \mathbf{z}^{1:k-1})$ can be evaluated via

$$p(\mathbf{z}^k \mid \mathbf{z}^{1:k-1}) = \int_{\mathbb{S}^{d-1}} p(\mathbf{z}^k \mid \mathbf{x}^k)p(\mathbf{x}^k \mid \mathbf{z}^{1:k-1})d\mathbf{x}^k. \tag{15}$$

The goal of the present paper is to employ the filtering equations (13), (14) and (15) when the underlying distributions are all of the vMF form. If these equations were to be solved for the Gaussian distribution, the result would be the Kalman filter [44].

If we assume that both the posterior at $k-1$ and the transition density are vMF distribution then the prediction step (13) would not yield another vMF distribution and the filtering equations would not stay in the domain of the same distribution. To solve this problem, a moment-matching technique is applied where the moments of the resulting distribution are matched to the moments of the corresponding vMF distribution. This procedure is also the optimal choice in the sense of the Kullback-Leibler divergence [45].

Let the state have the estimated position (direction) $\boldsymbol{\mu}^{k-1} \in \mathbb{S}^{d-1}$, conditioned upon all available measurements up to (and including) time $k-1$, which is statistically described by the density

$$p(\mathbf{x}^{k-1} \mid \mathbf{z}^{1:k-1}) = C_d(\kappa^{k-1})\exp(\kappa^{k-1}\boldsymbol{\mu}^{k-1}\cdot\mathbf{x}^{k-1}).$$

Calculating the directional mean with respect to the prediction density

$$\begin{aligned}\mathbb{E}[\mathbf{x}^k \mid \mathbf{z}^{1:k-1}] &= \int_{\mathbb{S}^{d-1}} \mathbf{x}^k p(\mathbf{x}^k \mid \mathbf{z}^{1:k-1})d\mathbf{x}^k \\ &= A_d(\kappa_\tau)A_d(\kappa^{k-1})\boldsymbol{\mu}^{k-1},\end{aligned}$$

and according to (5) we determine a unique vMF $f(\mathbf{x}^k;\bar{\boldsymbol{\mu}}^k,\bar{\kappa}^k)$ such that $\mathbb{E}[\mathbf{x}^k \mid \mathbf{z}^{1:k-1}] = A_d(\bar{\kappa}^k)\bar{\boldsymbol{\mu}}^k$. Thus, the prediction equations are

$$\bar{\boldsymbol{\mu}}^k = \boldsymbol{\mu}^{k-1}, \qquad \bar{\kappa}^k = A_d^{-1}(A_d(\kappa_\tau)A_d(\kappa^{k-1})), \tag{16}$$

where A_d^{-1} denotes the inverse to the function A_d defined in (6). To compute the inverse, one must resort to numerical methods since the derived equations are transcendental. Please see Proposition A.2 in Appendix A for the proof. Similar equations were derived in [13], [15], [16], [28], [29] for the cases of $d = 2$ and $d = 3$, i.e. for the distributions on the unit 1-sphere and the unit 2-sphere.

Upon availability of the measurement $\mathbf{z}^k$ at time k, and under the assumption that the sensor model follows the vMF density $f(\mathbf{z}^k;\mathbf{x}^k,\kappa_o)$, the posterior is found using the Bayes rule (14)

$$p(\mathbf{x}^k \mid \mathbf{z}^{1:k}) = C_d(\kappa^k)\exp(\kappa^k\boldsymbol{\mu}^k\cdot\mathbf{x}^k),$$

with corresponding update equations [29]

$$\begin{aligned}\kappa^k &= \|\kappa_o\mathbf{z}^k + \bar{\kappa}^k\bar{\boldsymbol{\mu}}^k\|, \\ \boldsymbol{\mu}^k &= \frac{\kappa_o\mathbf{z}^k + \bar{\kappa}^k\bar{\boldsymbol{\mu}}^k}{\kappa^k}.\end{aligned} \tag{17}$$

The Bayes normalizer (15) evaluates to

$$p(\mathbf{z}^k \mid \mathbf{z}^{1:k-1}) = \frac{C_d(\kappa_o)C_d(\bar{\kappa}^k)}{C_d(\kappa_k)}. \tag{18}$$

REMARK 2.1: The update equations of the 1-sphere Bayes filter, i.e. the von Mises filter [13], [15], [16], are

$$\kappa^k = \sqrt{\kappa_o^2 + (\bar{\kappa}^k)^2 + 2\kappa_o\bar{\kappa}^k\cos(\beta^k - \bar{\alpha}^k)}, \tag{19}$$

$$\alpha^k = \bar{\alpha}^k + \arctan\frac{\sin(\beta^k - \bar{\alpha}^k)}{\bar{\kappa}^k/\kappa_o + \cos(\beta^k - \bar{\alpha}^k)}, \tag{20}$$

where $\bar{\kappa}^k\bar{\boldsymbol{\mu}}^k = \bar{\kappa}^k(\cos\bar{\alpha}^k, \sin\bar{\alpha}^k)$ and $\kappa_o\mathbf{z}^k = \kappa_o(\cos\beta^k, \sin\beta^k)$. See Appendix A for the proof.

III. TRACKING IN CLUTTER WITH THE VON MISES-FISHER DISTRIBUTION

Target tracking in a cluttered environment requires, among other, to resolve the problem of measurement-to-target association. Moreover, in such approaches it is often practical to devise a validation gate so as to reject highly unlikely measurements. This way the computational complexity of the association procedure can be significantly lowered [1]. In this section we recall two basic probabilistic (nonbackscan) approaches, developed in seminal papers [46], [47] in the context of Poisson distributed clutter and models described by Gaussian distributions. Here we extend these approaches to directional (spherical) models described by vMF distributions.

A. Validation gating

In order to assess the validity of a measurement $\mathbf{z}^k$, we use the density (15) [48]. By inspecting (18) we can notice that the result of the integral does not have the form of a vMF distribution. If the goal was just to compute (18) for explicit values, we would not need to go further, but the validation gating assumes calculating confidence intervals which is inconvenienced by a non-standard density form of (18). To solve this issue, similar logic as in the prediction stage is used—in lieu of using the exact density, we will use the moment-matched vMF distribution. Given that, the directional mean with respect to (15) is

$$\begin{aligned}\mathbb{E}[\mathbf{z}^k \mid \mathbf{z}^{1:k-1}] &= \int_{\mathbb{S}^{d-1}} \mathbf{z}^k p(\mathbf{z}^k \mid \mathbf{z}^{1:k-1}) d\mathbf{z}^k \\ &= A(\bar{\kappa}^k)A(\kappa_o)\bar{\boldsymbol{\mu}}^k \end{aligned} \tag{21}$$

and according to (5) we determine a unique vMF $f(\mathbf{z}^k; \bar{\boldsymbol{\mu}}^k, \kappa_S^k)$ where

$$\kappa_S^k = A_d^{-1}(A_d(\kappa_o)A_d(\bar{\kappa}^k)). \tag{22}$$

Please confer Remark A.1 for the proof. Note that parameter κ_S^k has the role analogous to the Kalman innovation for linear models.

Having computed the required vMF density, we can determine the confidence intervals. When $d = 2$ the quantiles of the distribution with mean direction $\mu = 0$ are transferred to the linear interval $[-\pi, \pi]$ by cutting the unit circle at π. For an approximate validation region $100(1-\alpha)\%$, e.g. 95% when $\alpha = 0.05$, the lower and upper tail area are respectively defined as [28]

$$\begin{aligned}\Pr(-180 < x < -180 + \delta) &= \alpha/2, \\ \Pr(180 - \delta < x < 180) &= \alpha/2. \end{aligned} \tag{23}$$

When $d = 3$, an approximate $100(1-\alpha)\%$ validation region for $\mathbf{z}^k$ is [28]

$$\{\mathbf{z}^k : \mathbf{z}^k \cdot \bar{\boldsymbol{\mu}}^k \geq \cos\delta\}, \tag{24}$$

which defines the intersection of the unit 2-sphere with the cone having vertex at the origin, axis the mean direction $\bar{\boldsymbol{\mu}}^k$ and semi-vertical angle δ which is defined by

$$\Pr(\mathbf{z} \cdot \bar{\boldsymbol{\mu}}^k \geq \delta) = \alpha, \tag{25}$$

with $\mathbf{z}$ distributed according to vMF with parameters $\bar{\boldsymbol{\mu}}^k$ and κ_S. The tables linking desired validation regions defined by α, and for given concentration parameters κ the corresponding intervals defined by δ, can be found in [28], [49]. So the procedure is as follows, (i) specify the desired validation region, i.e. the α, (ii) given the computed κ_S from (22) and α by using tables we find the corresponding δ, (iii) we evaluate the obtained measurement $\mathbf{z}^k$ with respect to the predicted mean $\bar{\boldsymbol{\mu}}^k$ to see if it satisfies the validation region constraint, and (iv) if so the measurement is assigned to the target in question, otherwise it is considered as clutter.

B. Probabilistic data association filter

First we assume a single target in track with multiple measurements where the number of false alarms is a Poisson distributed random variable. Let Z^k denote the set of all measurements that fall within the validation gate at time k

$$Z^k = \{\mathbf{z}_j^k : j = 1, \ldots, m_k\},$$

and $Z^{1:k} = \{Z^1, \ldots, Z^k\}$ the history of all measurements within the validation gate. We want to calculate the conditional probability density $p(\mathbf{x}^k \mid Z^{1:k})$ for all $k \geq 1$. Assume that at a given time $k-1$, the object's direction is described by the vMF density

$$p(\mathbf{x}^{k-1} \mid Z^{1:k-1}) = C_d(\kappa^{k-1})\exp(\kappa^{k-1}\boldsymbol{\mu}^{k-1} \cdot \mathbf{x}^{k-1}).$$

Obtaining measurements Z^k we build the following set of hypotheses:

$$\mathcal{H}_j = \{\mathbf{z}_j^k \text{ is the correct measurement}\}, \quad j = 1, \ldots, m_k,$$

and

$$\mathcal{H}_0 = \{\text{none of the gated measurements are correct}\}.$$

Using the total probability formula, the posterior probability density at time k is given by

$$p(\mathbf{x}^k \mid Z^{1:k}) = \sum_{j=0}^{m_k} p(\mathbf{x}^k \mid \mathcal{H}_j, Z^{1:k}) P(\mathcal{H}_j \mid Z^{1:k}). \tag{26}$$

From the definition of $\mathcal{H}_j$ and using the Bayes rule, for $j = 1,\dots,m_k$ we have

$$\begin{aligned} p(\mathbf{x}^k \mid \mathcal{H}_j, Z^{1:k}) &= p(\mathbf{x}^k \mid \mathcal{H}_j, Z^k, Z^{1:k-1}) \\ &= \frac{p(Z^k, \mathcal{H}_j \mid \mathbf{x}^k) p(\mathbf{x}^k \mid Z^{1:k-1})}{p(Z^k, \mathcal{H}_j \mid Z^{1:k-1})} \\ &= \frac{p(\mathbf{z}_j^k \mid \mathbf{x}^k) p(\mathbf{x}^k \mid Z^{1:k-1})}{p(\mathbf{z}_j^k \mid Z^{1:k-1})}. \end{aligned} \tag{27}$$

Assuming that the likelihood and the prior density are both vMF with respective parameters $\mathbf{z}_j^k, \kappa_o$, and $\bar{\boldsymbol{\mu}}^k, \bar{\kappa}^k$ given by (16), then the posterior density in (27) is also vMF with parameters analogous to those in (17)

$$\kappa_j^k = \|\kappa_o \mathbf{z}_j^k + \bar{\kappa}^k \bar{\boldsymbol{\mu}}^k\|, \tag{28}$$

$$\boldsymbol{\mu}_j^k = \frac{\kappa_o \mathbf{z}_j^k + \bar{\kappa}^k \bar{\boldsymbol{\mu}}^k}{\kappa_j^k}, \quad j = 1,\dots,m_k. \tag{29}$$

Clearly, for $j = 0$, $p(\mathbf{x}^k \mid \mathcal{H}_0, Z^{1:k}) = p(\mathbf{x}^k \mid Z^{1:k-1})$.

Let $w_j = P(\mathcal{H}_j \mid Z^{1:k})$ denote the a posteriori probabilities of each feature having originated from the object in track. According to calculations in [47, Appendix]

$$w_j = \frac{p(\mathbf{z}_j^k \mid \mathcal{H}_j, Z^{1:k-1})}{b + \sum_{l=1}^{m_k} p(\mathbf{z}_l^k \mid \mathcal{H}_l, Z^{1:k-1})}, \quad j = 1,\dots,m_k, \tag{30}$$

$$w_0 = \frac{b}{b + \sum_{l=1}^{m_k} p(\mathbf{z}_l^k \mid \mathcal{H}_l, Z^{1:k-1})}, \tag{31}$$

where $b = c(1 - p_G p_D)/p_D$, $c > 0$ is the clutter density, p_G is the probability that the correct feature will be inside the validation gate, and p_D is the probability that the correct feature will be detected. Density $p(\mathbf{z}_j^k \mid \mathcal{H}_j, Z^{1:k-1})$ denotes the probability density of a measurement conditioned upon past data and hypothesis that is correct, which is assumed to be known and in our case it is modeled by the vMF density

$$p(\mathbf{z}_j^k \mid \mathcal{H}_j, Z^{1:k-1}) = f(\mathbf{z}_j^k; \bar{\boldsymbol{\mu}}^k, \kappa_S^k), \tag{32}$$

where κ_S^k is given by (22).

Having defined and calculated all the ingredients, posterior density (26) becomes a mixture of vMF densities

$$p(\mathbf{x}^k \mid Z^{1:k}) = \sum_{j=0}^{m_k} w_j f(\mathbf{x}^k; \boldsymbol{\mu}_j^k, \kappa_j^k). \tag{33}$$

In order to estimate the object's direction $\boldsymbol{\mu}^k \in \mathbb{S}^{d-1}$, we calculate the directional mean

$$\mathbb{E}[\mathbf{x}^k \mid Z^{1:k}] = \int_{\mathbb{S}^{d-1}} \mathbf{x}^k p(\mathbf{x}^k \mid Z^{1:k}) d\mathbf{x}^k = \sum_{j=0}^{m_k} w_j A_d(\kappa_j^k) \boldsymbol{\mu}_j^k,$$

and, using (5), determine the unique vMF density $f(\mathbf{x}^k; \boldsymbol{\mu}^k, \kappa^k)$, which is the best approximation of (33) in the sense of the Kullback-Leibler divergence by solving

$$\kappa^k = A_d^{-1}\left(\left\|\sum_{j=0}^{m_k} w_j A_d(\kappa_j^k) \boldsymbol{\mu}_j^k\right\|\right), \tag{34}$$

$$\boldsymbol{\mu}^k = \left(\sum_{j=0}^{m_k} w_j A_d(\kappa_j^k) \boldsymbol{\mu}_j^k\right) \Big/ A_d(\kappa^k). \tag{35}$$

The latter procedure is the analogon of computing the state estimate and covariance matrix from the mixture of Gaussians representing the posterior densities in [46], [47].

When $d = 2$, the expressions (34) and (35) need not be expressed in the vectorial form, but rather in the angular variables. Componentwise, they evaluate to the following formulae [50]

$$\begin{aligned} A_2^2(\kappa^k) &= \sum_{j=0}^{m_k} w_j^2 A_2^2(\kappa_j^k) \\ &\quad + 2 \sum_{\substack{j,i=1 \\ j<i}}^{m_k} w_j w_i A_2(\kappa_j^k) A_2(\kappa_i^k) \cos(\alpha_j^k - \alpha_i^k) \\ \tan \alpha^k &= \frac{\sum_{j=0}^{m_k} w_j A_2(\kappa_j^k) \sin \alpha_j^k}{\sum_{j=0}^{m_k} w_j A_2(\kappa_j^k) \cos \alpha_j^k}. \end{aligned} \tag{36}$$

C. Joint probabilistic data association filter

Next we consider the problem of tracking several interfering targets $\{\mathcal{O}_1,\dots,\mathcal{O}_N\}$, with the pertaining number being fixed to N. The main issue is how to appropriately assign features to targets in track. In principle, PDA filter approach could be applied for each object separately, but this would implicitly assume that all measurement features originated by another object in track are Poisson distributed clutter [47], and we would like to avoid such a rough assumption.

Let $\mathbf{X}^k = \{\mathbf{x}_1^k,\dots,\mathbf{x}_N^k\} \subset \mathbb{S}^{d-1}$ denotes the set of object's states (directions) at time k, and assume that at a given time $k-1$ position of each object $\mathcal{O}_i$ is described by the vMF density

$$p(\mathbf{x}_i^{k-1} \mid Z^{1:k-1}) = C_d(\kappa_i^{k-1}) \exp(\kappa_i^{k-1} \boldsymbol{\mu}_i^{k-1} \cdot \mathbf{x}_i^{k-1}).$$

Upon availability of a set of new measurements $Z^k = \{\mathbf{z}_j^k : j = 1,\dots,m_k\}$, the following set of hypotheses is built:

$$\mathcal{H}_{ij} = \{\mathbf{z}_j^k \text{ is caused by } \mathcal{O}_i\}, \quad j = 1,\dots,m_k,$$

and

$$\mathcal{H}_{i0} = \{\text{none of the measurements is caused by } \mathcal{O}_i\}.$$

Again, the total probability formula implies that the posterior density for object $\mathcal{O}_i$ at time k is given by

$$p(\mathbf{x}_i^k \mid Z^{1:k}) = \sum_{j=0}^{m_k} p(\mathbf{x}_i^k \mid \mathcal{H}_{ij}, Z^{1:k}) P(\mathcal{H}_{ij} \mid Z^{1:k}), \tag{37}$$

where densities $p(\mathbf{x}_i^k \mid \mathcal{H}_{ij}, Z^{1:k})$ are computed following the same lines and assumptions as in the previous PDA filter approach. They are vMF densities $f(\mathbf{x}_i^k; \boldsymbol{\mu}_{ij}^k, \kappa_{ij}^k)$ with parameters

$$\kappa_{ij}^k = \|\kappa_o \mathbf{z}_j^k + \bar{\kappa}_i^k \bar{\boldsymbol{\mu}}_i^k\|, \tag{38}$$

$$\boldsymbol{\mu}_{ij}^k = \frac{\kappa_o \mathbf{z}_j^k + \bar{\kappa}_i^k \bar{\boldsymbol{\mu}}_i^k}{\kappa_{ij}^k}, \quad j = 1, \ldots, m_k, \tag{39}$$

and $\kappa_{i0}^k = \bar{\kappa}_i^k$ and $\boldsymbol{\mu}_{i0}^k = \bar{\boldsymbol{\mu}}_i^k$.

The only difference between PDA filter and JPDA filter is in calculation of a posteriori association probabilities $w_{ij} = P(\mathcal{H}_{ij} \mid Z^{1:k})$, where JPDA filter takes into account measurement-to-object association events jointly across the set of objects. This means that hypothesis $\mathcal{H}_{ij}$ consists of all *valid joint association events* $\mathcal{E}$ which assign feature $\mathbf{z}_j^k$ to object $\mathcal{O}_i$. By valid joint association events we consider those which assert that every feature lying within the validation gate region can originate from at most one object and every object can generate at most one feature. Thus, they partition the hypothesis $\mathcal{H}_{ij}$ and

$$w_{ij} = \sum_{\mathcal{E} \in \mathcal{H}_{ij}} P(\mathcal{E} \mid Z^{1:k}), \quad j = 1, \ldots, m_k, \tag{40}$$

$$w_{i0} = 1 - \sum_{j=1}^{m_k} w_{ij}. \tag{41}$$

In order to compute $P(\mathcal{E} \mid Z^{1:k})$, two auxiliary indicator functions are introduced: *measurement association indicator* $\varphi_j(\mathcal{E})$, which indicates whether in event $\mathcal{E}$ measurement $\mathbf{z}_j^k$ is associated with any object, and *target detection indicator* $\delta_i(\mathcal{E})$, which indicates whether in $\mathcal{E}$ any measurement is associated with object $\mathcal{O}_i$. Following [47] and using vMF model instead of the Gaussian, we obtain

$$P(\mathcal{E} \mid Z^{1:k}) = B(\mathcal{E}) \prod_{\substack{l=1 \\ \varphi_l(\mathcal{E})=1}}^{m_k} f(\mathbf{z}_l^k; \bar{\boldsymbol{\mu}}_{i_l}^k, \kappa_{S,i_l}^k)$$

with $\kappa_{S,i_l}^k = A_d^{-1}(A_d(\kappa_o) A_d(\bar{\kappa}_{i_l}^k))$ analogous to (22), where i_l is the object index with which measurement $\mathbf{z}_l^k$ is associated. Next,

$$B(\mathcal{E}) = \frac{c^{\phi(\mathcal{E})}}{p_G^{\alpha(\mathcal{E})} C} \prod_{\substack{i=1 \\ \delta_i(\mathcal{E})=1}}^{N} p_D^i \prod_{\substack{i=1 \\ \delta_i(\mathcal{E})=0}}^{N} (1 - p_D^i),$$

where $\phi(\mathcal{E})$ is the number of false features in joint event $\mathcal{E}$, which is assumed Poisson distributed, $\alpha(\mathcal{E}) = \sum_{j=1}^{m_k} \varphi_j(\mathcal{E})$ is the number of measurement-to-object associations in $\mathcal{E}$, p_G is the probability that the correct measurement will be inside the validation gate, p_D^i is the detection probability of object $\mathcal{O}_i$, and C is the normalization constant.

Posterior density (37) for object $\mathcal{O}_i$ is again a mixture of vMF densities, and the estimated posterior direction $\boldsymbol{\mu}_i^k$ with uncertainty κ_i^k is calculated via

$$\kappa_i^k = A_d^{-1}\left(\left\|\sum_{j=0}^{m_k} w_{ij} A_d(\kappa_{ij}^k) \boldsymbol{\mu}_{ij}^k\right\|\right), \tag{42}$$

$$\boldsymbol{\mu}_i^k = \left(\sum_{j=0}^{m_k} w_{ij} A_d(\kappa_{ij}^k) \boldsymbol{\mu}_{ij}^k\right) \Big/ A_d(\kappa_i^k). \tag{43}$$

Here also for the case when $d = 2$, the resulting parameters can be computed as in (36).

IV. SYNTHETIC DATA EXPERIMENTS

In order to test the performance of the vMF PDA and JPDA filters, we have simulated the system for 250 time steps with maneuvering targets on the unit 1-sphere and the unit 2-sphere. The targets were uniformly spawned and their dynamics was described by a constant angular velocity model, where the disturbance acted as random noise in the angular acceleration. The number of spawned targets was a random integer from [3,5] for the JPDA case, while for the PDA case it was set to one. Since the JPDA filter assumes a constant and known number of targets in the scene, the originally spawned number of objects was kept constant during the simulation, i.e. there were no target births nor deaths. Please recall that the vM filter is the Bayes filter on the unit 1-sphere, while the vMF filter is the Bayes filter on the unit 2-sphere. The underlying motivation behind these simulations is MTT with directional sensors like microphone arrays and omnidirectional cameras. The former can determine directions to the sound sources based on microphone pair signal differences [15], [51], [52], while for the latter it has been shown that the image formation can be described by the unified spherical projection model yielding a representation of the omnidirectional image on the unit 2-sphere [30], [53], [54].

In order to make the simulations as realistic as possible (i) the trajectories were corrupted with the von Mises, i.e. the von Mises-Fisher noise, with concentration parameter $\kappa = 1500$,[2] (ii) the probability of detection was $p_D = 0.95$ and (iii) false alarms were simulated as a Poisson process on the unit spheres with the mean value $\lambda = \beta\mu(\mathbb{S}^{d-1})$, where μ denotes the area measure on $\mathbb{S}^{d-1}$, and the intensity $\beta = 0.25$ was defined as the number of false measurements per solid radian. For the 1-sphere case $\mu(\mathbb{S}^{d-1}) = 2\pi$, while for the 2-sphere case $\mu(\mathbb{S}^{d-1}) = 4\pi$. For example, on average we could expect $4\pi\beta$ false alarms per sensor frame sampled from a uniform distribution on the unit 2-sphere. For all the experiments the validation gate was computed for $\alpha = 0.01$, i.e. the validation region of 99% was used. The experiments involving the PDA and the JPDA filter were envisaged so as to simulate tracking of a single target and

[2]For the vM distribution this corresponds approximately to $\sigma = 1.5°$ [16], while for the vMF distribution it is closer to $\sigma = 1.8°$.

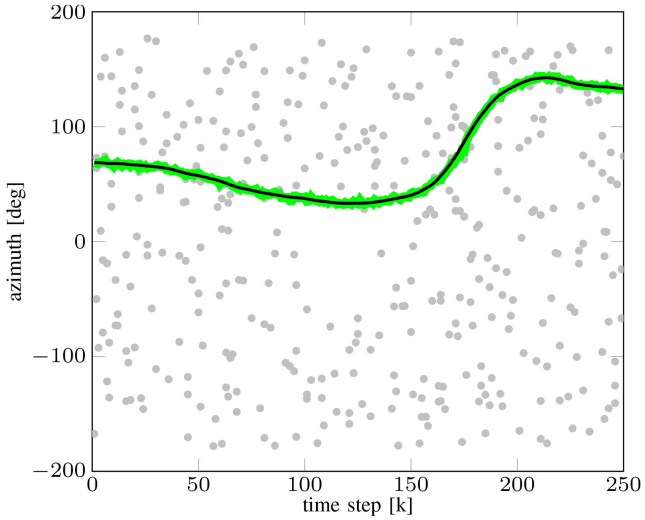

Fig. 3. An example of the experimental results of the tracking task for the von Mises PDA filter. The solid green line represents the estimated azimuth, while the solid black line is the ground truth. The gray circles represent false alarms. The mean error for this example was 0.97°.

multiple targets in clutter, both on the unit 1-sphere and the unit 2-sphere. In the end, we have performed 100 Monte Carlo runs of the previously described scenarios for both the vM and the vMF PDA and JPDA filters.

For the 1-sphere case the error Δ_{err} was computed as the absolute angular error by taking the periodicity into account

$$\Delta_{\text{err}} = |\text{mod}(\mathbf{x}_{\text{g}} - \mathbf{x}^k + \pi, 2\pi) - \pi|. \tag{44}$$

For the 2-sphere case the error Δ_{err} was computed as the great circle distance between the ground truth $\mathbf{x}_{\text{g}}$ and the estimated state $\mathbf{x}^k$

$$\Delta_{\text{err}} = \arccos(\mathbf{x}_{\text{g}} \cdot \mathbf{x}^k). \tag{45}$$

The expression (45) would yield the same result as (44) if therein 2D unit vectors were used instead of angles.

For the PDA filter the error calculation is straightforward, since we have only one object in the scene. But for the JPDA filter the error calculation cannot be approached in the same manner since we are tracking multiple objects and a ground truth trajectory needs to be paired up with a vMF filter trajectory. In this paper we are assuming known and constant number of objects in the scene, and, furthermore, we are focusing on deriving the fundamentals for probabilistic data association techniques on the unit hyperspheres. Hence, more involved methods for track management are not discussed in the present paper and in error calculation we are not penalizing if filters switches tracks when the two tracks cross. Therefore, for the JPDA filter case, we first calculate errors between all the filters and the ground truth trajectories, after which we apply the Hungarian algorithm [55], [56] to optimally assign filters to the ground truth trajectories. However, in Section IV-A we discuss solutions

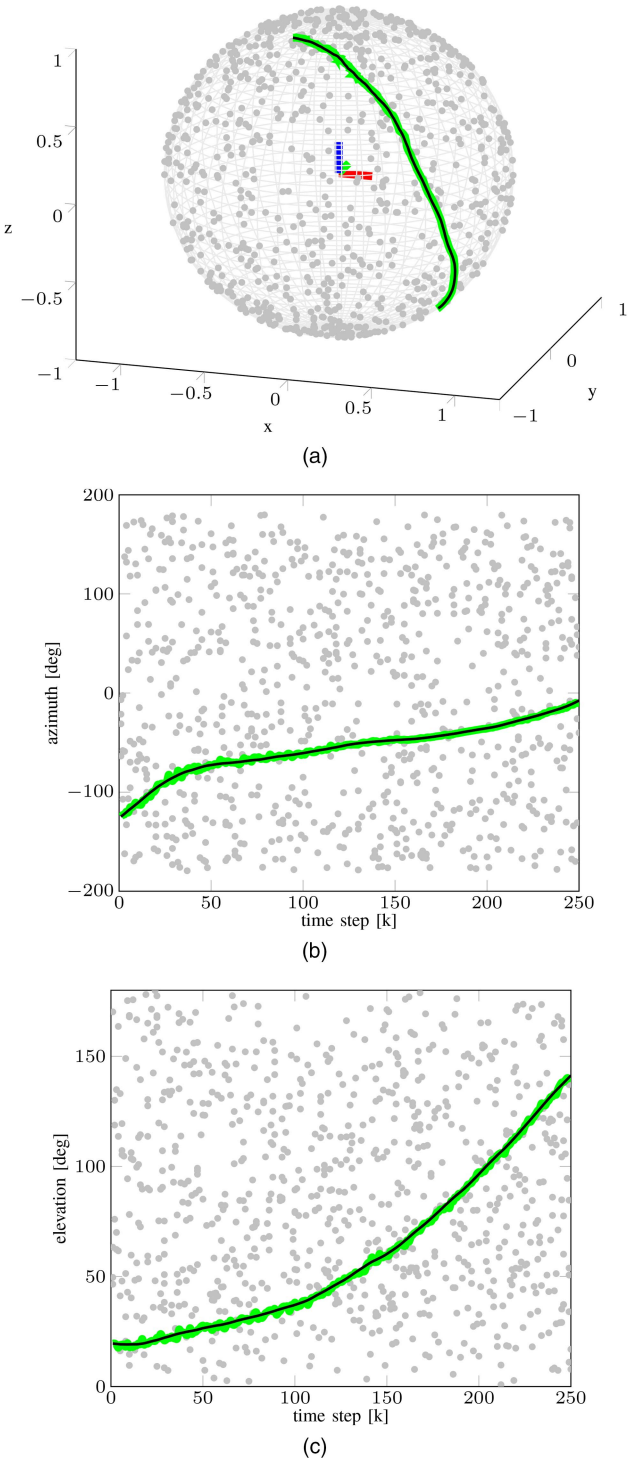

Fig. 4. An example of the experimental results of the tracking task for the vMF PDA filter. The solid green line represents the estimated direction, while the solid black line is the ground truth. The gray circles represent false alarms. The mean error for this example was 0.93°. (a) Trajectory on the unit 2-sphere. (b) Azimuth. (c) Elevation.

which could be applied for handling such multitarget tracking issues and metrics that can capture such errors.

Examples of the experimental results of the tracking task involving the PDA filter on the 1-sphere and the 2-sphere are shown in Figs. 3 and 4, respectively.

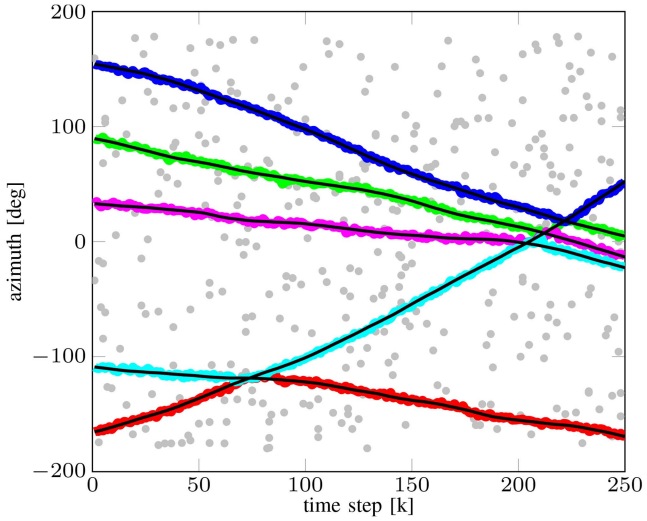

Fig. 5. An example of the experimental results of tracking five objects with the von Mises JPDA filter. The solid color lines represent the estimated azimuths, while the solid black lines are the ground truth. The gray circles represent false alarms. The mean absolute angular error of all the trajectories for this example was 0.99°.

The figures depict the ground truth, the estimated trajectory and false alarms. We can notice that the filters successfully manage to track the object in such a high clutter scenario, while yielding a mean error smaller than 1°. Figures 5 and 6 show an example of the JPDA filter tracking task. Examples with five objects in the scene are depicted, each color representing a single filter. We can see that in both cases filters manage to successfully track all the objects in the scene while maintaining overall mean error smaller than 1°. We can notice that the filters achieve mean error smaller than the measurement noise even when clutter is present. However, Fig. 5 deserves further comment. We can notice therein that during track crossing the filters switched tracks, e.g. at approximately 70 s the red and the cyan filter exchanged objects appearing as if they changed their course, while in truth they kept the same course during the whole simulation. As discussed previously, in the present paper we are not penalizing the track-switch, but we will address in Section IV-A how these issues can be alleviated.

Results of the 100 MC runs are depicted in Fig. 7. Therein statistics of the resulting errors is given both for the vM and vMF PDA and JPDA filters. The error for each run was calculated using (44) and (45) for the vM and the vMF filter, respectively. From the figure we can notice that the vM JPDA filter exhibited more outliers in comparison to others, but this was due to track coalescence. Namely, trajectories crossed much more often in the $[0, 2\pi]$ interval than they did on the unit 2-sphere. Overall, the median error was smaller than 1°.

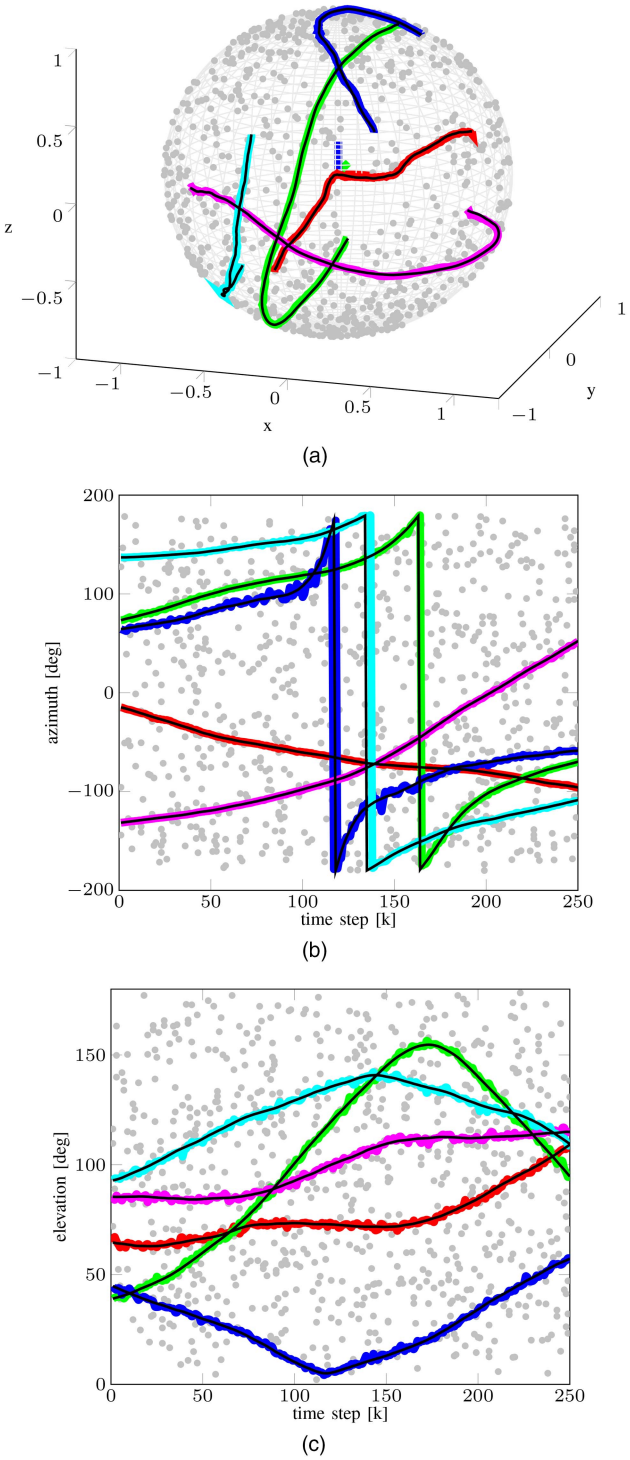

Fig. 6. An example of the experimental results of the tracking task for the vMF JPDA filter. The solid color lines represent the estimated directions, while the solid black lines are the ground truth. The gray circles represent false alarms. The mean error of all the trajectories for this example was 0.89°. (a) Trajectories on the unit 2-sphere. (b) Azimuth. (c) Elevation.

A. Discussion

As previously mentioned, the JPDA filter assumes known and constant number of objects in the scene. However, in [57] the joint integrated probability data association (JIPDA) filter was proposed in order to al-

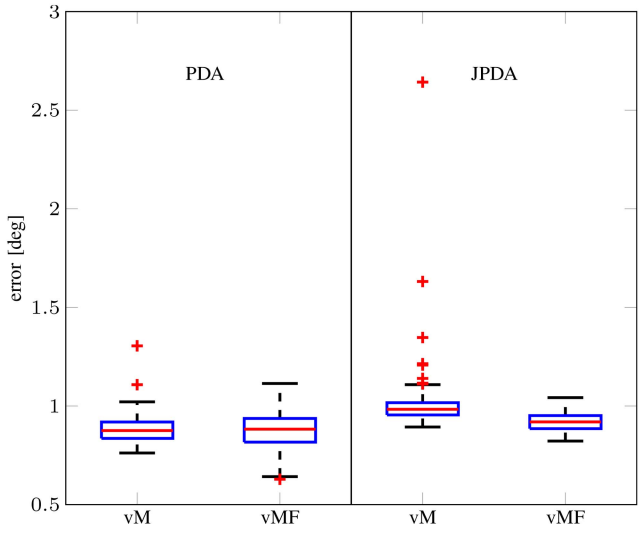

Fig. 7. Matlab's boxplot of the PDA and JPDA vM and vMF filter errors over 100 MC runs. The red lines are the median, the edges of the boxes are the 25th and 75th percentile, while the whiskers extend to the most extreme error not considered outliers and outliers are plotted as red pluses (errors 1.5 times larger than the difference between the percentiles).

leviate the JPDA assumption of the constant and known number of targets in the scene by including the probability of target existence within the framework. The results presented in this paper can be directly employed within the JIPDA framework. Furthermore, to handle issues like track switching and track coalescence, various other extensions of the PDA/JPDA filtering have been proposed [1], [58]. As long as the theoretical results derived in this paper are used, we believe that the aforementioned extensions can be applied to the vM and vMF JPDA filter as well.

In the present paper the likelihood for track switching is increased since the system state comprises of just the static component. If dynamical terms were included, the switch would be less likely to occur since terms like the estimated velocity would suggest the future motion of the object and would resolve situations like the one depicted in Fig. 5. However, principally including velocity components, which are in general Euclidean and not directional variables, into the same filtering framework is not a trivial task and is out of the scope of this paper. Examples of how the system state could be extended in this vein for the cases of the Bingham, vM and vMF distributions are given in [21], [26], [33], respectively.

Another solution for reducing the likelihood of track switch and coalescence is to include independent features for describing the tracked objects. For example, in multiple speaker tracking with a microphone array the fundamental frequency can tracked [59] and used in the data association process. When tracking moving objects with an omnidirectional camera appearance-based features can used to describe each object, like the HOG descriptor [60], which could also be used in the data association process. With these extensions at hand the multitarget tracking performance with respect to track switch, track loss, track coalescence and similar issues could be evaluated using the CLEAR MOT metrics [61], the optimal subpattern assignment metric [62] and its extensions [63], [64].

V. CONCLUSION

In the present paper we have proposed methods for tracking single and multiple targets in clutter on the $(d-1)$-sphere with the von Mises-Fisher distribution. The methods are based on Bayesian tracking and the data association logic of the PDA and JPDA filters. For single target tracking we have derived the PDA filter equations by assuming a moving object in a Poisson distributed clutter. This has resulted with a mixture of hypotheses represented as hyperspherical von Mises-Fisher densities which were weighted by the a posteriori probability that the selected measurement is correct. For multiple object tracking the JPDA filter was derived under similar assumptions which again resulted with a mixture of hypotheses represented as hyperspherical von Mises-Fisher densities, where each component was weighted by the a posteriori probability of the association event. The final single component estimate for each object in track, both in the PDA and JPDA filter case, was obtained by preserving the first moment of the distribution which is optimal in the Kullback-Leibler sense. For the cases of $d = 2$ and $d = 3$ the hyperspherical filter yields the vM PDA and JPDA and the vMF PDA and JPDA filter, respectively. In the end, the proposed methods were validated on synthetic data examples in 100 MC runs simulating scenarios of tracking a single and multiple targets in clutter on the unit 1-sphere and the unit 2-sphere.

APPENDIX A

PROPOSITION A.1 *The directional angular mean of the von Mises-Fisher density $f(\mathbf{x};\boldsymbol{\mu},\kappa)$ defined on $\mathbb{S}^{d-1}$ equals*

$$\mathbb{E}[\mathbf{x}] = \nabla F_d(\boldsymbol{\theta}) = A_d(\kappa)\boldsymbol{\mu}, \tag{46}$$

where $A_d(\kappa) = I_{d/2}(\kappa)/I_{d/2-1}(\kappa)$.

PROOF The first equality in (46) follows from the identity

$$0 = \int_{\mathbb{S}^{d-1}} (\mathbf{x} - \nabla F_d(\boldsymbol{\theta}))e^{\mathbf{x}\cdot\boldsymbol{\theta}-F_d(\boldsymbol{\theta})}d\mathbf{x},$$

obtained by differentiating $1 = \int_{\mathbb{S}^{d-1}} e^{\mathbf{x}\cdot\boldsymbol{\theta}-F_d(\boldsymbol{\theta})}d\mathbf{x}$ with respect to $\boldsymbol{\theta}$. For the second equality, using $\boldsymbol{\theta} = \kappa\boldsymbol{\mu}$ and $\|\boldsymbol{\theta}\| = \kappa$, we straightforwardly calculate

$$\nabla F_d(\boldsymbol{\theta}) = -\frac{C_d'(\kappa)}{C_d(\kappa)}\boldsymbol{\mu}. \tag{47}$$

Using the basic recurrence relations for the modified Bessel functions one obtains

$$C_d'(\kappa) = -\frac{\kappa^{d/2-1}}{(2\pi)^{d/2}}\frac{I_{d/2}(\kappa)}{I_{d/2-1}^2(\kappa)},$$

which yields

$$-\frac{C_d'(\kappa)}{C_d(\kappa)} = \frac{I_{d/2}(\kappa)}{I_{d/2-1}(\kappa)} =: A_d(\kappa).$$

PROPOSITION A.2 *Let the prior and the transition density be defined as following von Mises-Fisher densities*

$$\begin{aligned} p(\mathbf{x}^k \mid \mathbf{x}^{k-1}) &= f(\mathbf{x}^k; \mathbf{x}^{k-1}, \kappa_\tau) \\ p(\mathbf{x}^{k-1} \mid \mathbf{z}^{1:k-1}) &= f(\mathbf{x}^{k-1}; \boldsymbol{\mu}^{k-1}, \kappa^{k-1}). \end{aligned} \tag{48}$$

Then the directional mean of the predicted density $p(\mathbf{x}^k \mid \mathbf{z}^{1:k-1})$ *equals to*

$$\mathbb{E}[\mathbf{x}^k \mid \mathbf{z}^{1:k-1}] = A_d(\kappa_\tau) A_d(\kappa^{k-1}) \boldsymbol{\mu}^{k-1}. \tag{49}$$

PROOF The result is obtained by applying the Fubini's theorem (rearranging the terms within the integrals) and using the previous proposition:

$$\begin{aligned} &\mathbb{E}[\mathbf{x}^k \mid \mathbf{z}^{1:k-1}] \\ &= \int_{\mathbb{S}^{d-1}} \mathbf{x}^k \left(\int_{\mathbb{S}^{d-1}} p(\mathbf{x}^k \mid \mathbf{x}^{k-1}) p(\mathbf{x}^{k-1} \mid \mathbf{z}^{1:k-1}) d\mathbf{x}^{k-1} \right) d\mathbf{x}^k \\ &= \int_{\mathbb{S}^{d-1}} p(\mathbf{x}^{k-1} \mid \mathbf{z}^{1:k-1}) \left(\int_{\mathbb{S}^{d-1}} \mathbf{x}^k p(\mathbf{x}^k \mid \mathbf{x}^{k-1}) d\mathbf{x}^k \right) d\mathbf{x}^{k-1} \\ &= A_d(\kappa_\tau) \int_{\mathbb{S}^{d-1}} \mathbf{x}^{k-1} p(\mathbf{x}^{k-1} \mid \mathbf{z}^{1:k-1}) d\mathbf{x}^{k-1} \\ &= A_d(\kappa_\tau) A_d(\kappa^{k-1}) \boldsymbol{\mu}^{k-1}. \end{aligned} \tag{50}$$

A von Mises-Fisher distribution $f(\mathbf{x}^k; \bar{\boldsymbol{\mu}}^k, \bar{\kappa}^k)$ with matched moments then has parameters

$$\bar{\boldsymbol{\mu}}^k = \boldsymbol{\mu}^{k-1}, \qquad \bar{\kappa}^k = A_d^{-1}(A_d(\kappa_\tau) A_d(\kappa^{k-1})). \tag{51}$$

REMARK A.1: Observe that the same calculations as above yield the following. If the sensor likelihood and the predicted density are defined as the von Mises-Fisher densities

$$\begin{aligned} p(\mathbf{z}^k \mid \mathbf{x}^k) &= f(\mathbf{z}^k; \mathbf{x}^k, \kappa_o) \\ p(\mathbf{x}^k \mid \mathbf{z}^{1:k-1}) &= f(\mathbf{x}^k; \bar{\boldsymbol{\mu}}^k, \bar{\kappa}^k), \end{aligned} \tag{52}$$

then the directional mean of the Bayes normalizer $p(\mathbf{z}^k \mid \mathbf{z}^{1:k-1})$ evaluates to

$$\mathbb{E}[\mathbf{z}^k \mid \mathbf{z}^{1:k-1}] = A(\kappa_o) A(\bar{\kappa}^k) \bar{\boldsymbol{\mu}}^k. \tag{53}$$

PROOF OF REMARK 2.1. The equation (19) for κ^k follows directly from calculating the norm of the vector $\kappa_o \mathbf{z}^k + \bar{\kappa}^k \bar{\boldsymbol{\mu}}^k$. The proof of (20) is more involved, but also straightforward. First observe that

$$\alpha^k = \arctan \frac{\kappa_o \sin \beta^k + \bar{\kappa}^k \sin \bar{\alpha}^k}{\kappa_o \cos \beta_k + \bar{\kappa}^k \cos \bar{\alpha}^k}. \tag{54}$$

This form of the angle update is also frequently used [13], [16], but we find the expression (20) more expository from the prediction-correction standpoint [15]. Let us now transform the numerator in (54) as follows

$$\begin{aligned} &\kappa_o \sin \beta^k + \bar{\kappa}^k \sin \bar{\alpha}^k \\ &\quad = \kappa_o \sin(\nu^k + \bar{\alpha}^k) + \bar{\kappa}^k \sin \bar{\alpha}^k \\ &\quad = (\bar{\kappa}^k + \kappa_o \cos \nu^k) \sin \bar{\alpha}^k + \kappa_o \sin \nu^k \cos \bar{\alpha}^k, \end{aligned} \tag{55}$$

where $\nu^k = \beta^k - \bar{\alpha}^k$. Now using the trigonometric identity

$$A \sin x + B \cos x = \sqrt{A^2 + B^2} \sin\left(x + \arctan \frac{B}{A} \right),$$

we get the following formula

$$\begin{aligned} &\kappa_o \sin \beta^k + \bar{\kappa}^k \sin \bar{\alpha}^k \\ &\quad = \sqrt{\kappa_o^2 + (\bar{\kappa}^k)^2 + 2\kappa_o \bar{\kappa}^k \cos \nu^k} \\ &\qquad \cdot \sin\left(\bar{\alpha}^k + \arctan \frac{\sin \nu^k}{\bar{\kappa}^k / \kappa_o + \cos \nu^k} \right). \end{aligned} \tag{56}$$

Analogous procedure can be performed for the denominator of (54), yielding an expression similar to (56), where the corresponding sines are replaced by cosines. Returning to (54) cancels the square root terms and a tangent is left due to the sine and cosine ratio—yielding finally the sought mean angle update formula (20).

REFERENCES

[1] S. Blackman and R. Popoli
Design and Analysis of Modern Tracking Systems.
Artech House Publishers, 1999.

[2] Y. Bar-Shalom and E. Tse
Sonar tracking of multiple targets using joint probabilistic data association filter,
Automatica, vol. 11, pp. 451–460, 1975.

[3] D. Reid
An algorithm for tracking multiple targets,
IEEE Transactions on Automatic Control, vol. 24, no. 6, pp. 843–854, 1979.

[4] R. P. S. Mahler
Multitarget Bayes filtering via first-order multitarget moments,
IEEE Transactions on Aerospace and Electronic Systems, vol. 39, no. 4, pp. 1152–1178, oct 2003.

[5] K. Panta, D. E. Clark, and B.-N. Vo
Data association and track management for the Gaussian mixture probability hypothesis density filter,
IEEE Transactions on Aerospace and Electronic Systems, vol. 45, no. 3, pp. 1003–1016, 2009.

[6] B.-N. Vo and W.-K. Ma
The Gaussian mixture probability hypothesis density filter,
IEEE Transactions on Signal Processing, vol. 54, no. 11, pp. 4091–4104, nov 2006.

[7] R. Mahler
PHD filters of higher order in target number,
IEEE Transactions on Aerospace and Electronic Systems, vol. 43, no. 4, pp. 1523–1543, 2007.

[8] B.-T. Vo, B.-N. Vo, and A. Cantoni
Analytic implementations of the cardinalized probability hypothesis density filter,
IEEE Transactions on Signal Processing, vol. 55, no. 7, pp. 3553–3567, jul 2007.

[9] R. Mahler
Statistical Multisource-Multitarget Information Fusion.
Arthech House, 2007.

[10] B. T. Vo, B. N. Vo, and A. Cantoni
The cardinality balanced multi-target multi-Bernoulli filter and its implementations,
IEEE Transactions on Signal Processing, vol. 57, no. 2, pp. 409–423, 2009.

[11] S. Reuter, B. T. Vo, B. N. Vo, and K. Dietmayer
The labeled multi-Bernoulli filter,
IEEE Transactions on Signal Processing, vol. 62, no. 12, pp. 3246–3260, 2014.

[12] H. Deusch, S. Reuter, and K. Dietmayer
The labeled multi-Bernoulli SLAM filter,
IEEE Signal Processing Letters, vol. 22, no. 10, pp. 1561–1565, 2015.

[13] M. Azmani, S. Reboul, J.-B. Choquel, and M. Benjelloun
A recursive fusion filter for angular data,
in *IEEE International Conference on Robotics and Biomimetics (ROBIO)*, dec 2009, pp. 882–887.

[14] I. Marković and I. Petrović
Speaker localization and tracking with a microphone array on a mobile robot using von Mises distribution and particle filtering,
Robotics and Autonomous Systems, vol. 58, no. 11, pp. 1185–1196, 2010.

[15] ———
Bearing-only tracking with a mixture of von Mises distributions,
in *IEEE/RSJ International Conference on Intelligent Robots and Systems (IROS)*, 2012, pp. 707–712.

[16] G. Kurz, I. Gilitschenski, and U. D. Hanebeck
Recursive monlinear filtering for angular data based on circular distributions,
in *American Control Conference (ACC)*, 2013, pp. 5439–5445.

[17] G. Kurz, F. Faion, and U. D. Hanebeck
Constrained object tracking on compact one-dimensional manifolds based on directional statistics,
in *International Conference on Indoor Positioning and Indoor Navigation (IPIN)*, oct 2013, pp. 1–9.

[18] J. Traa and P. Smaragdis
A wrapped Kalman filter for azimuthal speaker tracking,
IEEE Signal Processing Letters, vol. 20, no. 12, pp. 1257–1260, 2013.

[19] D. F. Crouse, R. W. . Osborne, K. Pattipati, P. Willett, and Y. Bar-Shalom
Efficient 2D location estimation of sensor arrays using targets of opportunity,
Journal of Advances in Information Fusion, vol. 8, no. 1, pp. 73–89, 2013.

[20] D. F. Crouse
Maximum-likelihood post-detection radar ambiguity resolution,
IEEE Transactions on Aerospace and Electronic Systems, vol. 50, no. 3, pp. 1876–1883, 2014.

[21] G. Stienne, S. Reboul, M. Azmani, J. Choquel, and M. Benjelloun
A multi-temporal multi-sensor circular fusion filter,
Information Fusion, vol. 18, pp. 86–100, jul 2014.

[22] F. Pfaff, G. Kurz, and U. D. Hanebeck
Multimodal circular filtering using Fourier series,
in *International Conference on Information Fusion (FUSION)*, 2015, pp. 711–718.

[23] J. Glover, G. Bradski, and R. B. Rusu
Monte Carlo pose estimation with quaternion kernels and the Bingham distribution,
in *Proceedings of Robotics: Science and Systems*, Los Angeles, CA, USA, 2011.

[24] G. Kurz, I. Gilitschenski, S. Julier, and U. D. Hanebeck
Recursive estimation of orientation based on the Bingham distribution,
in *International Conference on Information Fusion (FUSION)*, 2013, pp. 1–16.

[25] ———
Recursive Bingham filter for directional estimation involving 180 degree symmetry,
Journal of Advances in Information Fusion, vol. 9, no. 2, pp. 90–105, 2014.

[26] J. Glover and L. P. Kaelbling
Tracking the spin on a ping pong ball with the quaternion Bingham filter,
in *IEEE International Conference on Robotics and Automation (ICRA)*, 2014, pp. 4133–4140.

[27] I. Gilitschenski, G. Kurz, S. J. Julier, and U. D. Hanebeck
Unscented orientation estimation based on the Bingham distribution,
IEEE Transactions on Automatic Control, vol. in press, p. 11, 2015.

[28] K. V. Mardia and P. E. Jupp
Directional Statistics.
Wiley, 1999.

[29] A. Chiuso and G. Picci
Visual tracking of points as estimation on the unit sphere,
in *The confluence of vision and control*, ser. Lecture Notes in Control and Information Sciences, D. Kriegman, G. Hager, and A. Morse, Eds. Springer London, 1998, vol. 237, pp. 90–105.

[30] I. Marković, F. Chaumette, and I. Petrović
Moving object detection, tracking and following using an omnidirectional camera on a mobile robot,
in *International Conference on Robotics and Automation (ICRA)*, 2014.

[31] J. Ćesić, I. Marković, and I. Petrović
Tracking of multiple moving objects on the unit sphere using a multiple-camera system on a mobile robot,
in *Internatinal Conference on Intelligent Autonomous Systems (IAS)*, 2014, p. 12.

[32] I. Marković, J. Ćesić, and I. Petrović
Von Mises mixture PHD filter,
IEEE Signal Processing Letters, vol. 22, no. 12, pp. 2229–2233, 2015.

[33] J. Traa and P. Smaragdis
Multiple speaker tracking with the factorial von Mises-Fisher filter,
in *IEEE International Workshop on Machine Learning for Signal Processing*, 2014.

[34] I. Marković, M. Bukal, J. Ćesić, and I. Petrović
Direction-only tracking of moving objects on the unit sphere via probabilistic data association,
in *International Conference on Information Fusion (FUSION)*, 2014, pp. 1–7.

[35] K. V. Mardia and P. E. Jupp
Directional statistics.
Wiley, 1999.

[36] F. Nielsen and V. Garcia
"Statistical exponential families: A digest with flash cards,"
arXiv:0911.4863, 2009.

[37] S. R. Jammalamadaka and A. Sengupta
Topics in Circular Statistics.
World Scientific, 2001.

[38] A. Banerjee
Clustering on the unit hypersphere using von Mises-Fisher distributions,
Journal of Machine Learning Research, vol. 6, pp. 1–39, 2005.

[39] A. H. Jazwinski
Stochastic processes and filtering theory.
New York: Academic press, 1970.

[40] K. Yosida
Brownian motion on the surface of the 3-sphere,
Ann. Math. Statist., vol. 20, no. 2, pp. 292–296, 1949.

[41] P. H. Roberts and H. D. Ursel
Random Walk on a Sphere and on a Riemannian Manifold,
Philosophical Transactions of the Royal Society of London. Series A, Mathematical and Physical Sciences, vol. 252, no. 1012, pp. 317–356, 1960.

[42] G. S. Watson
Statistics on Spheres.
Wiley, 1983.

[43] F. Beichlet
Stochastic Processes in Science, Engineering, and Finance. Chapman & Hall, 2006.

[44] S. Thrun, W. Burgard, and D. Fox
Probabilistic Robotics.
The MIT Press, 2006.

[45] O. Schwander and F. Nielsen
Learning mixtures by simplifying kernel density estimators,
in *Matrix Information Geometry*, F. Nielsen and R. Bhatia, Eds. Springer Berlin Heidelberg, 2013, pp. 403–426.

[46] Y. Bar-Shalom and T. Edison
Tracking in a cluttered environment with probabilistic data association,
Automatica, vol. 11, no. 5, pp. 451–460, 1975.

[47] T. Fortmann, Y. Bar-Shalom, and M. Scheffe
Sonar tracking of multiple targets using joint probabilistic data association,
IEEE Journal of Oceanic Engineering, vol. 8, no. 3, pp. 173–184, 1983.

[48] T. Bailey, B. Upcroft, and H. Durrant-Whyte
Validation gating for non-linear non-Gaussian target tracking,
in *International Conference on Information Fusion*, 2006, pp. 1–6.

[49] J. P. Marques de Sá
Applied Statistics using SPSS, Statistica, Matlab and R.
Springer-Verlag, 2007.

[50] M. Bukal, I. Marković, and I. Petrović
Composite distance based approach to von Mises mixture reduction,
Information Fusion, vol. 20, pp. 136–145, 2014.

[51] J.-M. Valin, F. Michaud, and J. Rouat
Robust localization and tracking of simultaneous moving sound sources using beamforming and particle filtering,
Robotics and Autonomous Systems, vol. 55, no. 3, pp. 216–228, 2007.

[52] S. Argentieri, P. Danès, and P. Souères
"A survey on sound source localization in robotics: from binaural to array processing methods,"
Laboratory for Analysis and Architecture of Systems, The National Center for Scientific Research, Tech. Rep., 2014.

[53] C. Geyer and K. Daniilidis
A unifying theory for central panoramic systems and practical implications,
in *European Conference on Computer Vision (ECCV)*, 2000, pp. 445–461.

[54] P. J. Barreto and H. Araújo
Issues on the geometry of central catadioptric image formation,
in *Conference on Computer Vision and Pattern Recognition (CVPR)*, 2001, pp. 422–427.

[55] H. W. Kuhn
The Hungarian method for the assignement problem,
Naval Research Logistics Quarterly, vol. 2, pp. 83–97, 1955.

[56] J. Munkres
Algorithms for the assignment and transportation problems,
Journal of the Society for Industrial and Applied Mathematics, vol. 5, no. 1, pp. 32–38, 1957.

[57] D. Mušicki and R. Evans
Joint Integrated Probabilistic Data Association—JIPDA,
IEEE Transactions on Aerospace and Electronic Systems, vol. 40, no. 3, pp. 1093–1099, 2004.

[58] Y. Bar-Shalom and X. R. Li
Multitarget-Multisensor Tracking: Principles and Techniques.
Storrs, CT: YBS Publishing, 1995.

[59] M. Murase, S. Yamamoto, J.-M. Valin, K. Nakadai, K. Yamada, K. Komatani, T. Ogata, and H. G. Okuno
Multiple moving speaker tracking by microphone array on a mobile robot,
in *INTERSPEECH*, 2005, p. 4.

[60] A. A. Mekonnen, C. Briand, F. Lerasle, and A. Herbulot
Fast HOG based person detection devoted to a mobile robot with a spherical camera,
in *IEEE/RSJ International Conference on Intelligent Robots and Systems (IROS)*, nov 2013, pp. 631–637.

[61] K. Bernardin and R. Stiefelhagen
Evaluating multiple object tracking performance: The CLEAR MOT metrics,
EURASIP Journal on Image and Video Processing, vol. 2008, p. 10, 2008.

[62] D. Schuhmacher, B. T. Vo, and B. N. Vo
A consistent metric for performance evaluation of multi-object filters,
IEEE Transactions on Signal Processing, vol. 56, pp. 3447–3457, 2008.

[63] B. Ristic, B.-N. Vo, D. Clark, and B.-T. Vo
A metric for performance evaluation of multi-target tracking algorithms,
IEEE Transactions on Signal Processing, vol. 59, no. 7, pp. 3452–3457, 2011.

[64] T. Vu and R. Evans
A new performance metric for multiple target tracking based on optimal subpattern assignment,
in *International Conference on Information Fusion (FUSION)*, 2014, p. 8.

Ivan Marković received the B.Sc. and the Ph.D. degree in Electrical Engineering from the University of Zagreb, Faculty of Electrical Engineering and Computing (FER), Croatia in 2008 and 2014, respectively. He is currently employed at the FER, Zagreb, as a Postdoctoral fellow funded by the Ministry of Science, Education and Sport, Republic of Croatia. In 2014 he was awarded with the Silver Plaque "Josip Loncar" faculty award for outstanding doctoral dissertation and particularly successful scientific research. During his undergraduate studies, for outstanding academic achievements, he received the "Institute for Nuclear Technology Award" and the "Josip Loncar Award" in 2007 and 2006, respectively. In 2013 and 2014 he was a visiting researcher at Inria Rennes-Bretagne Atlantique in the Lagadic group directed by François Chaumette. He also serves as the coordinator of the technical editing team of the Automatika journal. His research interests are mobile robotics, estimation theory, especially detection and tracking of moving objects and speaker localization.

Mario Bukal received the M.S. degree in applied mathematics from the University of Zagreb, Faculty of Science in 2008 and the Ph.D. in applied mathematics from the Vienna University of Technology, Faculty of Mathematics and Geoinformation in 2012. From 2012 he is with the University of Zagreb, Faculty of Electrical Engineering and Computing, where he is a postdoctoral researcher working on several research projects. His research focus is in applied mathematics, in particular, mathematical and numerical analysis of diffusion equations and cross-diffusion systems, and homogenization and dimension reduction in nonlinear elasticity theory, but his research interests also include information fusion with applications to robotic systems.

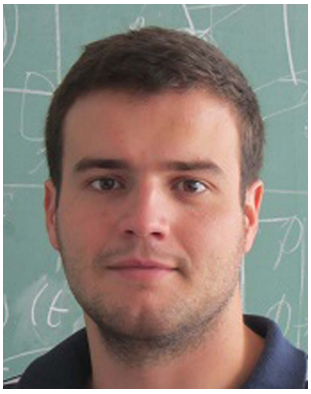

Josip Ćesić received his B.Sc. and M.Sc. degree (Magna Cum Laude) in electrical engineering and information technology from University of Zagreb, Faculty of Electrical Engineering and Computing (FER) in 2011 and 2013, respectively. He finished the third semester of his master program at Chalmers University of Technology, Sweden, as an exchange student. He received several scholarships and awards for outstanding achievements during his undergraduate and graduate studies. He works as a research fellow at the Department of Control and Computer Engineering at FER since April 2013. His main research interests are in the areas of autonomous systems and mobile robotics, estimation theory and sensor processing.

Ivan Petrović received B.Sc. degree in 1983, M.Sc. degree in 1989 and Ph.D. degree in 1998, all in Electrical Engineering from the Faculty of Electrical Engineering and Computing (FER), University of Zagreb, Croatia. He had been employed as an R&D engineer at the Institute of Electrical Engineering of the Končar Corporation in Zagreb from 1985 to 1994. Since 1994 he has been with FER, where he is currently a full professor. He teaches a number of undergraduate and graduate courses in the field of control systems and mobile robotics. His research interests include various advanced control strategies and their applications to control of complex systems and mobile robots navigation. He has published more than 40 journal and 160 conference papers, and results of his research have been implemented in several industrial products. He is a member of IEEE, IFAC—TC on Robotics and FIRA—Executive committee. He is a member of the Croatian Academy of Engineering and Editor-in-Chief of the Automatika journal.